

Feasibility of pseudocontinuous arterial spin labeling at 7 T with whole-brain coverage

Eidrees Ghariq · Wouter M. Teeuwisse ·
Andrew G. Webb · Matthias J. P. van Osch

Received: 1 June 2011 / Revised: 4 October 2011 / Accepted: 1 December 2011 / Published online: 27 December 2011
© The Author(s) 2011. This article is published with open access at Springerlink.com

Abstract

Object We studied the feasibility of pseudocontinuous arterial spin labeling (pCASL) at 7 T.

Materials and methods Simulations were performed to find the optimal labeling parameters for pCASL, with particular attention to the maximum-allowed specific absorption rate (SAR). Subsequently, pCASL experiments (four volunteers) were performed to find the B1 efficiency at the labeling position with and without high-permittivity pads placed around the head, and to study the optimal labeling duration (four separate volunteers). Finally, feasibility of whole-brain pCASL imaging was tested.

Results Simulations showed that a lower B1 efficiency should be compensated by a lower effective flip angle of the labeling, a moderately shorter labeling duration, and a longer repetition time. B1 efficiency in the internal carotid arteries just below the carotid siphon was approximately 55% and 35% with and without high-permittivity pads, respectively. In vivo experiments showed an optimal labeling duration of 1,500 ms, although longer labeling durations up to 2,500 ms resulted in similar signal-to-noise efficiency. Whole-brain pCASL imaging was demonstrated in a single volunteer.

Conclusion Despite decreased B1 efficiency, sufficient labeling efficiency can be achieved for whole-brain pCASL at 7 T with high-permittivity pads. However, image quality is still limited compared with 3 T, probably due to imaging instabilities, and further research is needed to elucidate this.

Keywords Cerebral blood flow · MRI · Cerebral arteries · Arterial spin labeling

Introduction

Cerebral perfusion, i.e., cerebral blood flow (CBF), is increasingly recognized as an important marker of cerebrovascular (dys)function. CBF measurements therefore play an increasingly important role in both the clinical and the research arena. Established clinical applications of perfusion imaging include acute stroke, intracranial tumors, and stenotic carotid artery disease [1–5]. Research applications of CBF measurements include calibration of functional magnetic resonance imaging (MRI) [e.g., quantitative blood oxygenation level dependent (BOLD) imaging], cerebrovascular reactivity measurements, and pharmacological MRI [6–8]. Arterial spin labeling (ASL) MRI is the only truly noninvasive technique for perfusion imaging. ASL employs arterial blood as an endogenous contrast agent and is based on subtraction of two consecutively acquired proton-density-weighted images. Prior to the first acquisition, the so-called label image, arterial blood is labeled upstream of the imaging slice by means of inversion or saturation of the magnetization of blood in the feeding arteries. After a short delay (1–2 s) that allows the labeled spins to flow to the microvasculature and to exchange with the tissue compartment, the label image is acquired. The second, or control, image is acquired under the same conditions but without blood labeling. Upon subtraction of the two images, the static tissue signal is cancelled, leaving a perfusion-weighted image.

Continuous ASL (CASL) has several advantages over other ASL implementations, with the main advantage being a long and well-defined duration of the bolus of labeled blood [9, 10]. Furthermore, when a CASL image is

E. Ghariq (✉) · W. M. Teeuwisse · A. G. Webb ·
M. J. P. van Osch

Department of Radiology, C.J. Gorter Center for High Field
MRI, Leiden University Medical Center (LUMC), C3-Q,
Albinstadweg 2, 2333 ZA Leiden, The Netherlands
e-mail: ghariq@lumc.nl

acquired with a postlabeling delay that is longer than the transport time of blood from the labeling slab to the imaging region, straightforward quantification of perfusion can be obtained. Due to the long labeling duration, CASL has a higher signal-to-noise ratio (SNR), especially at field strengths of 3 T and higher, compared with pulsed ASL (PASL) methods. The main disadvantages of CASL are the high demands put on the radiofrequency (RF) amplifier and the high specific absorption rate (SAR) associated with the long labeling pulse. To overcome these limitations, Garcia et al. proposed a modification of CASL, dubbed pCASL (for pulsed- or pseudocontinuous ASL) that splits the long RF pulse into a train of shorter RF pulses (typically 0.5 ms at a 1-ms interval), thereby lowering the demands on the RF amplifier [11, 12] while obtaining a higher labeling efficiency than multislice CASL [13]. Since its introduction, the pCASL technique has become, arguably, the most popular ASL technique due to the possibility of acquiring whole-brain, high SNR ASL scans in a relatively short scan time [14, 15]. An additional drawback of (p)CASL techniques compared with PASL is the fact that (p)CASL only offers information on CBF, whereas multi-T-I PASL techniques also provide measurement of timing parameters [16].

In recent years, all main MRI manufacturers have introduced ultra-high-field MRI scanners into their portfolio. When advocating ultra-high-field MRI, most people include ASL in their list of MRI techniques that will benefit most when going from medium (3 T) to ultra-high-field MRI (≥ 7 T). The potential benefits of higher field strength for ASL are at least threefold: (1) the inherent higher SNR at higher field strengths; (2) the increased longitudinal relaxation time (T_1) resulting in a slower label decay; (3) higher-field MRI and parallel imaging work synergistically, creating possibilities for increasing robustness of high sensitivity-encoding (SENSE) factors, enabling faster readout strategies at a higher spatial resolution [17]. However, initial experiments with ASL at ultra-high-field MRI showed that implementation of ASL and obtaining the expected gains at 7 T is not trivial [16, 18]. First, the fivefold increase in SAR at 7 T with respect to 3 T is an important challenge, possibly limiting the label duration or increasing the required repetition time of SAR-intensive ASL methods, such as CASL and pCASL, resulting in a lower SNR per unit time. Second, the increased B_0 magnetic field inhomogeneities pose problems for labeling, especially because these are most pronounced at the regions where this labeling has to take place for both PASL and (p)CASL methods. A third challenge is the B_1 inhomogeneity at 7 T due to the decreased electromagnetic wavelength in tissue, making the design and use of a body coil challenging, which has resulted in the common setup of using a much smaller

head coil for transmission. Together, these factors result in limited B_1 efficiency at the level of the brain-feedings arteries. A possible solution is to label higher in the brain, but this will immediately lead to a sacrifice of whole-brain coverage, a significant disadvantage compared with current practice at 3 T. Alternatively, it has been suggested that for such transmit coils, the use of pads with high permittivity material wrapped around the neck can improve B_1 at the level of labeling [19]. It is, however, uncertain whether this benefit is large enough to enable efficient labeling. Other limiting factors are the increased sensitivity to physiological noise at 7 T and a reduced transverse relaxation time (T_2).

Finally, several additional improvements in pCASL have been suggested by different groups [20, 21]. Most notably, incorporation of additional inversion pulses between the labeling module and the imaging sequence—the so-called background suppression pulses—has been shown to reduce physiological noise and improve ASL image quality at 3 T [21]. The overall effect of using these background suppression pulses for pCASL at 7 T is uncertain because of the increase in SAR that accompanies the addition of extra pulses and the associated decrease in temporal SNR (tSNR). Although the possible benefits that can be gained from the background suppression will be the subject of future research, the primary focus of this study was implementation of the balanced pCASL sequence at 7 T and optimization of this labeling module.

The aim of the study was to optimize the labeling module of the pCASL sequence for 7 T with regard to B_1 inhomogeneities without compromising whole-brain coverage of pCASL. To achieve this, the B_1 distribution for the most commonly used commercial transmit head coil was evaluated in vivo. The B_1 efficiency at the brain-feeding arteries was determined with and without dielectric pads around the neck of volunteers in order to study the effectiveness of this approach. Subsequently, theoretical models for pCASL were employed to determine optimal settings of labeling parameters to optimize SNR per unit time while staying within SAR limitations. Finally, pCASL images were obtained to prove the feasibility at ultra-high-field MRI.

Materials and methods

All experiments were performed on a 7-T Philips Achieva scanner (Philips Healthcare, Best, The Netherlands) using a quadrature birdcage transmit coil in combination with either a 16- or 32-channel receive head coil (all Nova Medical, Wilmington, MA, USA). Informed consent was obtained from all participants, and the study was approved by the local Institutional Review Board.

Numeric simulations

Numeric simulations were performed to obtain optimal settings for labeling parameters while staying within SAR limits. Simulations consisted of three modules: simulations to calculate the labeling efficiency of the pCASL-train, a general kinetic model to estimate the resulting perfusion signal, and an SAR module to ensure that the sequence would run in vivo on the 7-T MRI scanner. For parameter space, see Table 1.

Labeling efficiency of the pCASL train

Labeling efficiency of the balanced pCASL module was calculated by solving the Bloch equations numerically, similar to the setup described in Wu et al. [13]. In brief, blood magnetization was simulated flowing with a constant velocity of 20 cm/s through the labeling plane. Based on the slice profile of the Hanning-pulses and the simulated flip angle (FA), the effective FA at the location of the spin is calculated. Subsequently, the acquired phase due to the mean gradient in the slice-select direction is calculated, and the transverse magnetization is rotated accordingly. At the same time, T_1 and T_2 relaxation are taken into account (assuming a T_1 and T_2 of blood of 2.6 s and 54 ms, respectively [22]). Then, the distance travelled by blood between labeling pulses is calculated and the entire process repeated until blood exits the labeling slab.

General kinetic model

The general kinetic model as proposed by Buxton et al. was employed to estimate ASL signal as a function of labeling duration [23]. The T_1 of blood and tissue were assumed to be 2.6 s and 2.0 s, respectively [22]. Transport time from the labeling plane to the capillaries was assumed to be 1,450 ms at a CBF of 95 ml/100 ml/min based on values reported by Liu et al. [24]. A fixed-delay time between labeling and imaging of 1,500 ms (i.e., slightly longer than the assumed transport time) was used to achieve accurate quantification of CBF while maximizing SNR [9]. The model should be considered a first-order approximation of the ASL signal at ultra-high-field MRI because exchange

of labeled spins with tissue is assumed to be instantaneous. More realistic two-compartment models could be employed that take into account the gradual exchange of magnetization along capillaries [25–27]. Parkes et al. [25] previously demonstrated that this, in particular, changes the results for high perfusion values but that the influence for a simulated CBF of 95 ml/100 ml/min is negligible.

SAR model

In vivo experiments were used to determine how the labeling parameters affect the SAR of the total sequence and at what levels the 7-T MRI scanner would stop the execution of the sequence due to an excessive time-averaged SAR. As expected from theoretical considerations, this relation was linear with the labeling duration, quadratic with the FA of the pulses employed in the pCASL train, and inversely related to the time from one RF pulse of the train to the next (TR_{pCASL}). Based on this model, the sequence TR (TR_{sq}) was calculated for single-slice acquisition, i.e., the readout module consisted of only a single 90° RF pulse and should therefore be considered to reflect the minimal achievable SAR for an ASL acquisition.

To calculate optimal values for the pCASL sequence at 7 T, the parameter space was fixed by choosing specific intervals for the different parameters based on hardware limitations. B1 efficiency was defined as the effective FA as a percentage of the nominal FA after RF power optimization was performed at the imaging volume. Simulation parameters were varied within the following ranges: B1 efficiency 20–100%, nominal FA of the pCASL train pulses 5°–50°, pCASL repetition time (TR_{pCASL}) 1–2 ms, and labeling duration 1,000–5,000 ms. After initial experiments, the mean gradient strength was fixed at 0.6 mT/m and the TR_{pCASL} was fixed at 1.2 ms, because the influence on the result was very small. For each combination of parameter settings, labeling efficiency was calculated first, the SAR-allowed minimal TR_{sq} was subsequently determined, and finally, based on the general kinetic model, the resulting ASL signal was calculated. The settings that resulted in optimal temporal SNR as defined by the ASL signal divided by the square root of the TR_{sq} were calculated as a function of B1 efficiency.

In vivo measurements of B1 efficiency in arteries

To measure B1 efficiency in major arteries across the brain, so-called FA sweeps were performed in four healthy male volunteers (aged 22–37 years) at four different levels of the arterial vasculature (Fig. 2) using the 32-channel (three volunteers) and 16-channel (one volunteer) head coils, both with a SENSE factor of 2.5. Power optimization was performed at the brain tissue level to determine the amount of

Table 1 Mesh spacing and mesh sizes used for simulations

Parameter	Interval (step size)
B1 efficiency	20–100% (0.5%)
Nominal flip angle	5°–50° (0.05°)
TR_{pCASL}	1–2 ms (0.05 ms)
Label duration	1,000–5,000 ms (10 ms)

TR_{pCASL} pseudocontinuous arterial spin labeling repetition time

power needed for maximum signal, i.e., a 90° RF pulse. The same power settings were employed during labeling, resulting in a reduced effective FA for the RF pulses in the pCASL train due to the lower B1 efficiency of the transmit coil in the neck region. B1 efficiency was measured with a single-slice gradient-echo (GRE) sequences with a TR 250 ms and TE 3.3 ms [field of view (FOV) 220×181 mm, matrix size 224×179 , SENSE factor 2.5]. An FA sweep of $50\text{--}310^\circ$ (step size 20°) was applied for the excitation pulse. Assuming complete fresh inflow, arterial MRI signal shows a sinusoidal dependency as a function of the FA. The FA that renders maximum signal intensity (FA_{\max_s}) corresponds with an effective FA of 90° , and B1 efficiency can be calculated as $B_{1, \text{efficiency}} = (90^\circ/FA_{\max_s}) \times 100\%$.

The same experiments were repeated with high-permittivity pads placed around the neck of the participants to study the influence on B1 efficiency. Three dielectric pads were prepared and connected together. The central bag had dimensions of 12.5×17.5 cm, with two larger pads 18×17.5 cm on either side. These were joined together to form a combined size of 48.5×17.5 cm. A mixture of calcium titanate (Alfa Aesar) in deuterated water (99%) with weight ratio 3:1 was prepared and heat-sealed within the polypropylene pad after taking care to remove as much of the entrapped air as possible. Previous work has shown that this suspension has a high relative dielectric constant of ~ 110 at 298 MHz [19].

In vivo experiments to determine the influence of labeling duration on ASL signal

To validate simulations, four volunteers (two men and two women; age range 23–26 years) were scanned with eight different label durations: 500, 1,000, 1,500 ... 4,000 ms using the 16-channel head coil with a SENSE factor of 2.5 while keeping the SAR within limits, as determined by the SAR model of the scanner (necessitating an increase in TR as $TR \approx 655 \text{ ms} + 2.2 \times \tau$, τ being the labeling duration). Total acquisition time of all scans was kept constant, ~ 5 min, by reducing the number of dynamics, i.e., the number of label and control images (other labeling parameters: delay = 1,550 ms, gradient strength = 6 mT/m, mean gradient = 0.6 mT/m, RF duration = 0.5 ms, pulse repetition time $TR_{\text{pCASL}} = 1.2$ ms; echo planar imaging (EPI) readout with TE = 11.35 ms and fat suppression using a frequency-selective saturation pulse preceded the labeling pulses). Linear shim settings were determined for the labeling plane and imaging volume using standard preparation sequences as supplied by the vendor [28]. Furthermore, separate measurements of water resonance frequency (f_0) were performed for the labeling plane and imaging volume. For every individual a region of interest (ROI) was calculated by thresholding ($2.5 \times$ mean

over the positive perfusion values) on the ASL map averaged over all eight labeling durations. Mean signal and mean SNR per unit time (tSNR), or SNR efficiency, was calculated as a function of labeling duration.

Putting it all together: whole-brain pCASL at 7 T

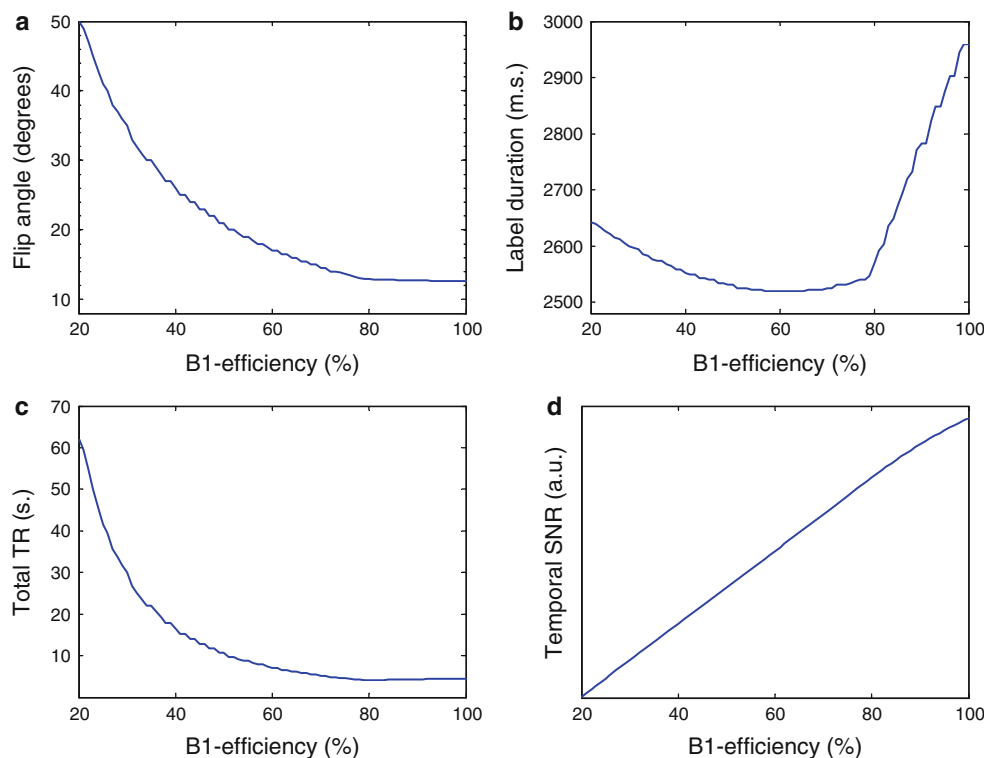
To confirm our theoretical predictions from numerical simulations, optimal settings were used in a healthy volunteer (26-year-old woman) with the dielectric pads in place using the 32-channel head coil (acceleration factor = 3.5). To calculate labeling efficiency in arteries prior to pCASL sequence, an FA sweep was acquired from which the B1 efficiency was calculated, as described above. In addition, a B1 map was acquired at the level of the brain tissue to determine the effective FA to correct the perfusion maps for the B1 inhomogeneity at tissue level. For this purpose, a 3D GRE scan was acquired applying the double-TR method, with a voxel size of $3 \times 3 \times 4$ mm, TR1/TR2/TE = 30/150/1.44 ms, FA 40° , 28 slices, and an image acquisition time of 3 min [29].

Results

Simulations

The first observation from the simulations was that, independent of B1 efficiency, the highest temporal SNR was obtained with the shortest possible pulse interval in the pCASL train (TR_{pCASL}), the limit of which is dependent on the hardware (results not shown). This is in agreement with the results reported by Dai et al. and could be explained by the fact that as the pulse repetition time increases, the number of pulses experienced by a fast-moving spin will decrease, reducing labeling efficiency. Accordingly, this was fixed at TR = 1.2 ms in further simulations. It appeared that SAR limits are more efficiently overcome by lowering the FA or the label duration than by increasing the interval between RF-train pulses. Similarly, and in line with the observation of a constant pulse interval, results revealed that the optimum mean gradient strength was around 0.6 mT/m, which did not vary considerably across the B1 efficiency space, so further simulations were conducted using a fixed value of 0.6 mT/m for this parameter. Figure 1a shows the optimum combination of FA of RF pulses of the pCASL labeling train and label duration as a function of B1 efficiency. For lower B1 efficiencies, the optimal temporal SNR can be achieved by increasing the nominal FA, i.e., compensating for the loss in B1, while lowering the label duration to stay within SAR limits. Decreases in label duration are, however, subtle, varying between 3,000 and 2,500 ms. When operating at a B1

Fig. 1 Settings of nominal flip angle (FA) (a), label duration (b), sequence repetition time (TR) (c) for optimal signal to noise ratio (SNR) per unit time as a function of B1 efficiency. Values are determined by combined numerical simulations of the labeling process, the general kinetic perfusion model, and a specific absorption rate (SAR) model of the 7-T MRI scanner. Resulting SNR per unit time (d). The following values were used for this simulation: pseudocontinuous arterial spin labeling repetition time (TR_{pCASL}) = 1.2 ms; mean gradient strength = 0.6 mT/m; cerebral blood flow (CBF) = 95 ml/100 ml/min; blood transit time from the labeling slab to the imaging slice = 1,450 ms; postlabeling delay = 1,500 ms, and blood velocity = 20 cm/s



efficiency of 45%, which can be considered the worst case for in vivo measurements, temporal SNR is more sensitive to a suboptimal nominal FA than to a change in labeling duration.

B1-efficiency mapping and effect of dielectric pads

Figure 2 shows an example of the B1-efficiency measurements in the large brain-feeding arteries. MRI signal strength is indicated as a function of FA (FA sweep graphs) for the right internal carotid artery at different levels along its trajectory. It is clear that B1 efficiency decreases significantly for positions below the carotid siphon, where one normally would like to label in order to achieve whole-brain coverage. Based on the determination of the FA leading to maximum signal intensity, B1 efficiency can be calculated for the arteries at different levels (see Fig. 3).

These results show that B1 efficiency rapidly declines when moving caudally. Furthermore, it shows that even at the most cranially studied position, efficiency is still <80%. In addition, efficiency can vary considerably between arteries at the same level. The effect of high-permittivity pads is an increase in B1 efficiency, especially at the more caudal positions, and a decrease in variation in B1 efficiency between arteries at the same level in the brain.

In vivo experiments

Figure 4a shows the dependence of the ASL signal in a single-slice pCASL acquisition as a function of labeling duration in a single volunteer. An improvement in image quality can be observed when increasing the labeling duration from 500 to 1,500 ms, but a further increase does not lead to further improvement. The averaged findings for all four volunteers are shown in Fig. 4b and c. Results show that the ASL signal increases with longer labeling durations, whereas this increase in the perfusion-weighted signal is not accompanied by an increase in temporal SNR (see Fig. 4c). This is probably caused by the rapidly increasing SAR, limiting the number of label and control image pairs that can be acquired in the set scan time of 5 min. The maximum SNR/unit time in these experiments was achieved for a labeling duration of 1,500 ms.

Whole-brain pCASL at 7 T

In a female volunteer of 26 years, whole-brain pCASL imaging was performed with pads of high dielectric material wrapped around the head. Before acquiring pCASL data, B1 efficiency was measured at the brain-feeding arteries just below the siphon, that is, at the

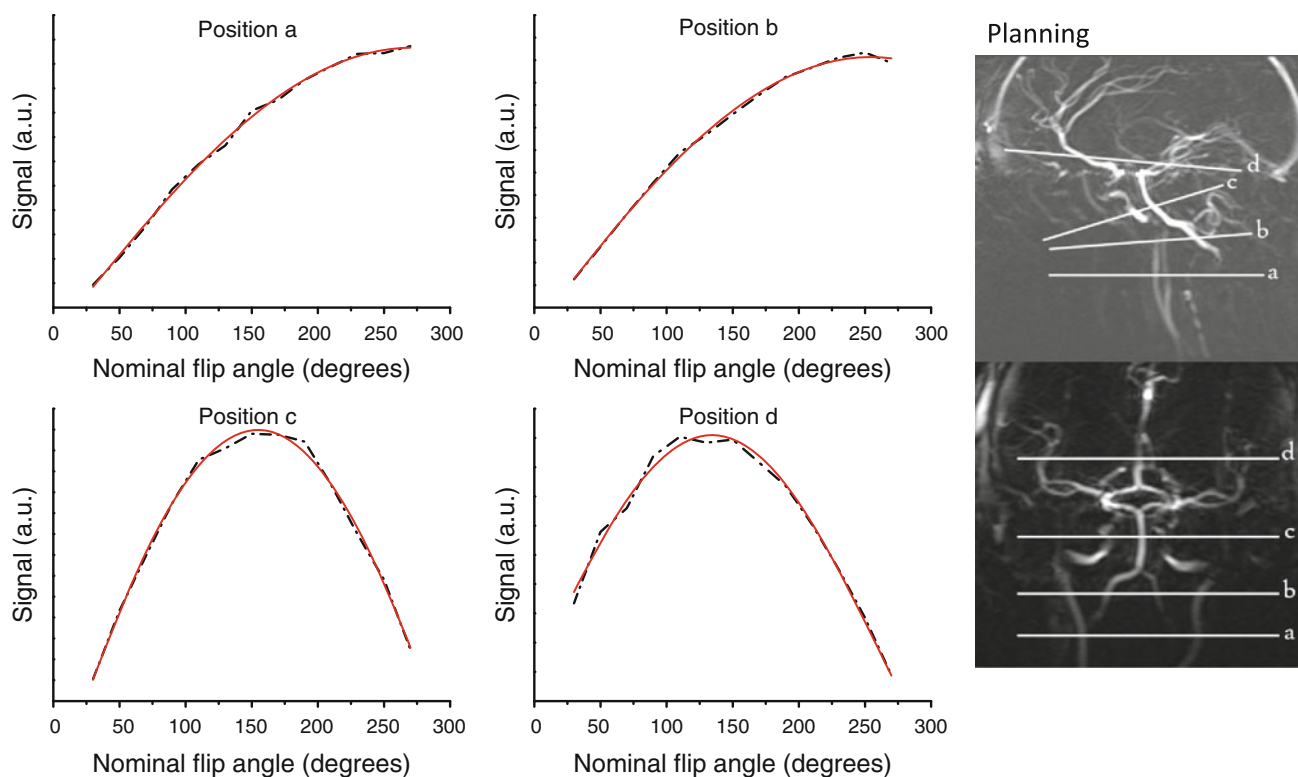


Fig. 2 Signal strength in the right internal carotid artery (position **a–c**) and right middle cerebral artery (position **d**) as a function of the nominal flip angle (FA) in a volunteer without high-permittivity pads present. When assuming complete fresh inflow, the position of maximum signal reflects an effective FA of 90° . In this example, B1

efficiency at the most cranial position is about 65% and drops below 35% inferior to the carotid siphon. The *dotted line* shows measured values, the *red lines* depicts the fitted curve from which the 90° effective FA was calculated. Distance between labeling locations **a** and **d** was approximately 9.5 cm on the coronal scan

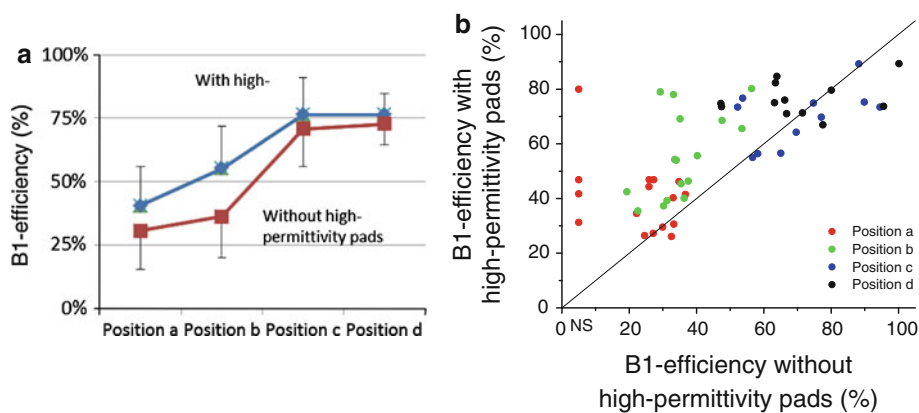


Fig. 3 B1 efficiency in the main brain-feeding arteries as measured at different levels with and without high-permittivity pads placed around the head of the volunteers. In the *left graph* (**a**), B1 efficiency as averaged over all arteries and four volunteers is shown for the anatomical levels shown in Fig. 2. These measurements show that placement of pads around the head of the volunteer increases B1

efficiency, especially in the most caudal positions. *Error bars* indicate standard deviation. The graph on the *right* (**b**) shows a scatter plot of B1 efficiency with dielectric pads versus B1 efficiency without the pads, demonstrating improved B1 efficiency. The *solid line* represents the $x = y$ axis

location where labeling is performed. These B1-efficiency measurements showed an average efficiency of approximately 50%. Subsequently, whole-brain pCASL imaging was performed, showing reasonably high labeling efficiency, although slightly different for different flow

territories (see Fig. 5). Furthermore, it should be noted that lower in the brain, in particular, there are some EPI-related imaging artifacts. This figure also shows B1 efficiency at the brain tissue level in combination with the correction factor that should be applied to the ASL images to correct

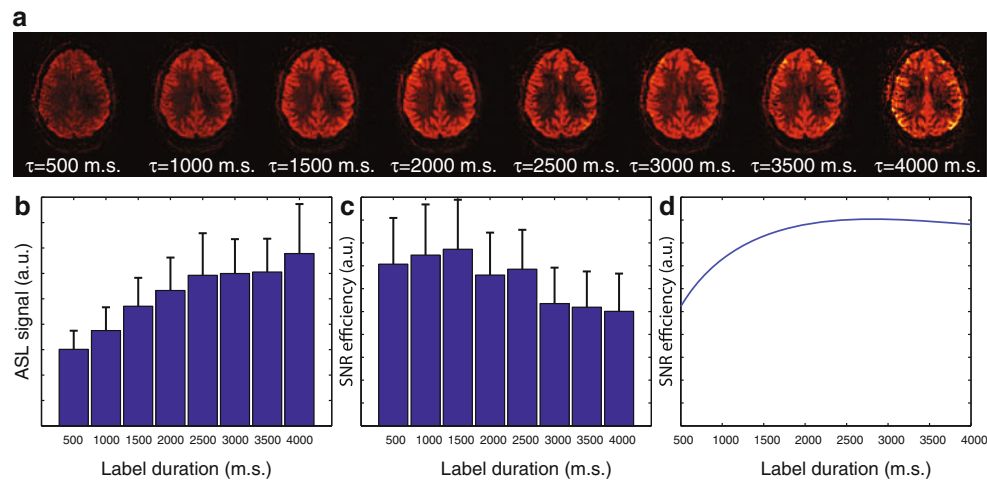


Fig. 4 Arterial spin labeling (ASL) signal and signal-to-noise ratio (SNR) efficiency as a function of labeling duration. *Top row*: mean ASL signal as a function of labeling duration (τ) as measured in a single volunteer. *Bottom row, from left to right*: ASL signal as function of labeling duration (τ) averaged over four volunteers;

temporal SNR as a function of labeling duration (τ); simulations of the temporal SNR as a function of label duration. [Pseudocontinuous arterial spin labeling repetition time (TR_{pCASL}) = 1.2 ms, flip angle = 18° , mean gradient = 0.8 mT/m, assumed B1 efficiency = 80%]

for FA variations across the brain. The influence of such a correction is, however, small, as is evident when comparing ASL images with and without B1 correction or when considering the different images.

Discussion

Whereas ASL is frequently quoted as one of the techniques that will benefit immensely by moving from 3 T to 7 T, initial experiences have proved that it is challenging to achieve these theoretical improvements. In this study, we focused on the balanced pCASL technique, as the ASL technique of choice at 3 T, and showed that, in particular, the lower B1 efficiency at the preferred location for labeling imposes significant challenges to achieving whole-brain ASL imaging at 7 T with an improved SNR compared with 3 T. Several factors affect the ability to achieve whole-brain pCASL at 7 T.

Labeling location

To achieve whole-brain coverage with pCASL, it is essential to label below the circle of Willis, because otherwise the labeling plane will intersect with the imaging slices, thereby corrupting ASL measurements. However, in this study, we show that B1 efficiency within the arteries drops from 80% just above the circle of Willis to $<35\%$ at approximately the location where labeling is performed at 3 T (see Figs. 2 and 3). Based on these findings, it could be argued that positioning the labeling plane at the level of the

basilar artery and just above the carotid siphon should be optimal. However, it has been shown previously that this region is very susceptible to magnetic field inhomogeneities, resulting in low labeling efficiencies [18]. This was also confirmed by our own feasibility experiments, which did not show high and/or consistent labeling efficiency at this labeling position. When aiming for whole-brain-coverage pCASL, it is therefore advised to position the labeling plane just below the carotid siphon (location b in Fig. 2), although this will result in a lower B1 efficiency for labeling.

B1 efficiency

When using a standard-transmit head coil at 7 T, B1 efficiency at the labeling plane will be limited, although positioning of high dielectric pads around the head can improve B1 efficiency considerably. This approach has previously been applied to imaging and spectroscopy in the human head at ultra high field [19, 30]. Use of the dielectric pads improved B1 efficiency at the optimal labeling position by almost 60%, thereby making whole-brain pCASL feasible. An alternative solution would be to use a separate labeling transmit coil, similar to CASL approaches at 3 T [31]. The use of a separate labeling coil involves, however, a more difficult hardware setup and, in particular, requires stringent safety procedures to limit SAR deposition in the neck region and coil isolation during the imaging readout. Furthermore, applicability of ASL in patient studies at 7 T would be limited if it required placement of an additional labeling coil due to decreased patient comfort.

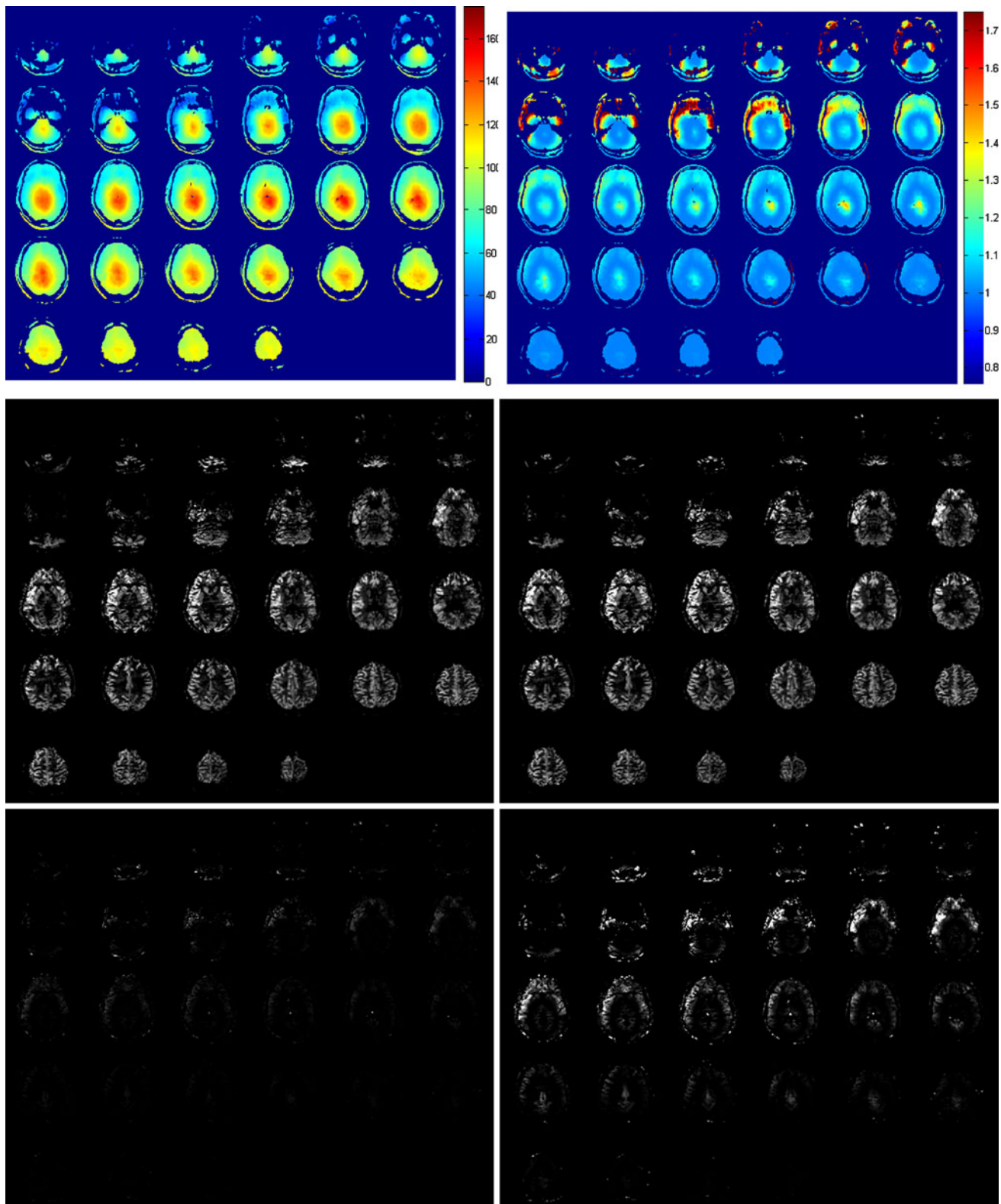


Fig. 5 In vivo measurements of B1 efficiency and whole-brain pseudocontinuous arterial spin labeling (pCASL) measured in a female volunteer of 26 years. *Top row*: B1 efficiency (%) *left* and resulting correction factor for arterial spin labeling (ASL) images (calculated as $1/\sin(90 \times \text{B1 efficiency}/100\%)$); *middle row*: ASL

image without (*left*) and with (*right*) correction for the inhomogeneous B1; *bottom row*: difference of ASL images with and without B1 correction at the same contrast as the original images (*left*) and displayed at a five-times higher contrast level (*right image*)

Optimal labeling parameters for SAR-constrained pCASL

Due to the long train of RF pulses that constitute the pCASL labeling module and the lower B1 efficiency at the labeling plane, pCASL is severely SAR-limited at 7 T. To comply with SAR restrictions, several approaches could be taken, among the most important of these being a longer interval between RF pulses, a shorter labeling duration, a decrease in TR_{seq} , and the use of a smaller-than-optimal effective FA. Based on simulations presented in this study, the interval between RF pulses should be chosen to be as short as possible, and SAR reduction should be achieved by a subtle interplay between smaller effective FAs and a shorter labeling duration in combination with an increased TR sequence to stay within SAR safety guidelines. When using these optimal settings, it should be noted that the temporal resolution of the ASL sequence is reduced, which can be an important disadvantage, especially when using ASL to detect neuronal activation. Another possibility to reduce the SAR is to increase FA duration, because the SAR scales quadratically with RF amplitude. This will, of course, change the slice profile of the Hanning pulses, and it remains to be studied how this would affect labeling efficiency.

Although the simulations were calculated for only a single blood velocity value (20 cm/s), it could be argued that the results are not limited by this. The choice for this value for simulations was partly based on results published by Dai et al. [11] showing that dependence of labeling efficiency on flow velocity is small when flow velocity is in the range of physiological values of 15–60 cm/s. This was also confirmed by our own unpublished experiments that justified the choice of the aforementioned value and reinforced the validity of the findings.

B0 shimming

In the pCASL implementation used in this study, a separate shimming procedure is performed at the labeling plane independent from the normal shimming of the imaging volume. This limits, however, both shimming procedures to linear gradients only, resulting in suboptimal shimming lower in the brain, as evidenced in Fig. 5. The use of higher-order shimming would certainly improve image quality lower in the brain and the use of dynamic shimming, i.e., the use of different higher-order shims for each imaging slice, would be even better, although only very few ultra-high-field MRI scanners currently have these capabilities [32, 33]. An important feature of the implementation used here is that a separate f_0 measurement is performed at the labeling plane, correcting for unwanted

phase variation over the labeling slice that would occur if using the same f_0 as determined for the imaging volume [34]. Without the use of dielectric pads, MRI signal in the labeling slice was too low in several study participants to obtain a proper shimming and f_0 determination at that location. With the dielectric pads, such problems were minimized, although a further signal increase could probably improve the shimming and f_0 determination considerably.

Readout module

When taking into account that reasonable labeling efficiency was achieved in our volunteer, as demonstrated in the upper slices in Fig. 5, it becomes evident that the poor imaging quality in the lower slices should be attributed to the readout module. In this study, a standard multislice EPI readout with parallel acceleration factor of 3.5 was used as the readout module, whereas alternative readout sequences might have helped improve the image quality. First, it should be noted that the excitation pulses necessary to acquire 30 slices add significantly to the total SAR of the sequence. Second, the use of 3D readout strategies has demonstrated large potential at 3 T, although the use of many refocusing pulses as applied in the gradient- and spin-echo (GRASE) MRI sequence is probably less optimal at 7 T [35]. Other readout options, such as 3D-EPI and fast low-angle shot (FLASH) should be evaluated at 7 T for their quality. Furthermore, in this study, no background suppression was employed, which would be expected to be beneficial by limiting the influence of physiological noise on the image quality, especially in the lower part of the brain. However, background suppression would make a significant contribution to the overall SAR sequence, leading to longer TR_{sq} and thus a reduced tSNR. For instance, in the case of this participant, each additional background suppression pulse was accompanied by an SAR increase of ~ 0.1 W/kg, necessitating an additional increase in TR_{sq} of 500 ms to stay within the scanner's SAR limits.

B1 inhomogeneities at the imaging slice

Inhomogeneous distribution of the RF in the brain is a well-known problem at 7 T. The influence on ASL maps is, however, limited. As can be seen in Fig. 5, the influence is mainly in the lower parts of the brain, where image quality is already limited due to poor shimming and physiological noise. Qualitative differences between ASL images with and without correction for spatial FA variations in this study were too small to be quantified, except for a very slight change in the center of the brain.

Conclusion

Obtaining high enough labeling efficiency, i.e., ASL signal with a high SNR efficiency, at 7 T for whole-brain pCASL MRI is feasible, but only when pads of high-permittivity material wrapped around the patient's head are used and by increasing the TR of the sequences to remain within SAR limits. Furthermore, the multislice EPI readout resulted in significant image artifacts lower in the brain. More research needs to be done, especially focusing on improving the readout module and inclusion of background suppression to make 7-T ASL an alternative to 3-T pCASL.

Open Access This article is distributed under the terms of the Creative Commons Attribution Noncommercial License which permits any noncommercial use, distribution, and reproduction in any medium, provided the original author(s) and source are credited.

References

1. Wu O, Christensen S, Hjort N, Dijkhuizen RM, Kucinski T, Fiehler J, Thomalla G, Röther J, Østergaard L (2006) Characterizing physiological heterogeneity of infarction risk in acute human ischaemic stroke using MRI. *Brain* 129:2384–2393
2. Hendrikse J, van Osch MJP, Rutgers DR, Bakker CJG, Kappelle LJ, Golay X, van der Grond J (2004) Internal carotid artery occlusion assessed at pulsed arterial spin-labeling perfusion MR imaging at multiple delay times. *Radiology* 233: 899–904
3. Griebel J, Mayr NA, de Vries A, Knopp MV, Gneiting T, Kremser C, Essig M, Hawighorst H, Lukas PH, Yuh WT (1997) Assessment of tumor microcirculation: a new role of dynamic contrast MR imaging. *J Magn Reson Imaging* 7:111–119
4. Essig M, Weber M-A, von Tengge-Kobligk H, Knopp MV, Yuh WTC, Giesel FL (2006) Contrast-enhanced magnetic resonance imaging of central nervous system tumors: agents, mechanisms, and applications. *Top Magn Reson Imaging* 17:89–106
5. Lin W, Celik A, Derdeyn C, An H, Lee Y, Videen T, Ostergaard L, Powers WJ (2001) Quantitative measurements of cerebral blood flow in patients with unilateral carotid artery occlusion: a PET and MR study. *J Magn Reson Imaging* 14:659–667
6. Uludağ K, Dubowitz DJ, Yoder EJ, Restom K, Liu TT, Buxton RB (2004) Coupling of cerebral blood flow and oxygen consumption during physiological activation and deactivation measured with fMRI. *NeuroImage* 23:148–155
7. Bokkers RPH, van Osch MJP, van Der Worp HB, de Borst GJ, Mali WPTM, Hendrikse J (2010) Symptomatic carotid artery stenosis: impairment of cerebral autoregulation measured at the brain tissue level with arterial spin-labeling MR imaging. *Radiology* 256:201–208
8. Khalili-Mahani N, van Osch MJP, Baerends E, Soeter RP, de Kam M, Zoethout RWM, Dahan A, van Buchem MA, van Gerwen JMA, Rombouts SARB (2011) Pseudocontinuous arterial spin labeling reveals dissociable effects of morphine and alcohol on regional cerebral blood flow. *J Cereb Blood Flow Metab* 31:1321–1333
9. Alsop DC, Detre JA (1996) Reduced transit-time sensitivity in noninvasive magnetic resonance imaging of human cerebral blood flow. *J Cereb Blood Flow Metab* 16:1236–1249
10. Wong EC, Buxton RB, Frank LR (1998) A theoretical and experimental comparison of continuous and pulsed arterial spin labeling techniques for quantitative perfusion imaging. *Magn Reson Med* 40:348–355
11. Dai W, Garcia DM, de Bazelaire C, Alsop DC (2008) Continuous flow-driven inversion for arterial spin labeling using pulsed radio frequency and gradient fields. *Magn Reson Med* 60:1488–1497
12. Garcia DM, de Bazelaire C, Alsop DC (2005) Pseudo-continuous flow driven adiabatic inversion for arterial spin labeling. In: *Proceedings of the 13th annual meeting of ISMRM, Miami Beach, FL, USA*, p 37 (Abstract 39)
13. Wu W-C, Fernández-Seara MA, Detre JA, Wehrli FW, Wang J (2007) A theoretical and experimental investigation of the tagging efficiency of pseudocontinuous arterial spin labeling. *Magn Reson Med* 58:1020–1027
14. van Osch MJP, Teeuwisse WM, van Walderveen MAA, Hendrikse J, Kies DA, van Buchem MA (2009) Can arterial spin labeling detect white matter perfusion signal? *Magn Reson Med* 62:165–173
15. Fernández-Seara MA, Edlow BL, Hoang A, Wang J, Feinberg DA, Detre JA (2008) Minimizing acquisition time of arterial spin labeling at 3T. *Magn Reson Med* 59:1467–1471
16. Gardener AG, Gowland PA, Francis ST (2009) Implementation of quantitative perfusion imaging using pulsed arterial spin labeling at ultra-high field. *Magn Reson Med* 61:874–882
17. Wiesinger F, Van de Moortele P-F, Adriany G, De Zanche N, Ugurbil K, Pruessmann KP (2006) Potential and feasibility of parallel MRI at high field. *NMR Biomed* 19:368–378
18. Teeuwisse WM, Webb AG, van Osch MJP (2010) Arterial spin labeling at ultra-high field: All that glitters is not gold. *Int J Imaging Syst Technol* 20:62–70
19. Haines K, Smith NB, Webb AG (2010) New high dielectric constant materials for tailoring the B1 + distribution at high magnetic fields. *J Magn Reson* 203:323–327
20. Nezamzadeh M, Matson GB, Young K, Weiner MW, Schuff N (2010) Improved pseudo-continuous arterial spin labeling for mapping brain perfusion. *J Magn Reson Imaging* 31:1419–1427
21. Garcia DM, Duhamel G, Alsop DC (2005) Efficiency of inversion pulses for background suppressed arterial spin labeling. *Magn Reson Med* 54:366–372
22. Rooney WD, Johnson G, Li X, Cohen ER, Kim S-G, Ugurbil K, Springer CS (2007) Magnetic field and tissue dependencies of human brain longitudinal 1H2O relaxation in vivo. *Magn Reson Med* 57:308–318
23. Buxton RB, Frank LR, Wong EC, Siewert B, Warach S, Edelman RR (1998) A general kinetic model for quantitative perfusion imaging with arterial spin labeling. *Magn Reson Med* 40:383–396
24. Liu P, Uh J, Lu H (2011) Determination of spin compartment in arterial spin labeling MRI. *Magn Reson Med* 127:120–127
25. Parkes LM, Tofts PS (2002) Improved accuracy of human cerebral blood perfusion measurements using arterial spin labeling: accounting for capillary water permeability. *Magn Reson Med* 48:27–41
26. St Lawrence KS, Frank JA, McLaughlin AC (2000) Effect of restricted water exchange on cerebral blood flow values calculated with arterial spin tagging: a theoretical investigation. *Magn Reson Med* 44:440–449
27. Zhou J, Wilson DA, Ulatowski JA, Traystman RJ, van Zijl PC (2001) Two-compartment exchange model for perfusion quantification using arterial spin tagging. *J Cereb Blood Flow Metab* 21:440–455
28. Schär M, Kozerke S, Fischer SE, Boesiger P (2004) Cardiac SSFP imaging at 3 Tesla. *Magn Reson Med* 51:799–806
29. Yarnykh VL (2007) Actual flip-angle imaging in the pulsed steady state: a method for rapid three-dimensional mapping of the transmitted radiofrequency field. *Magn Reson Med* 57:192–200
30. Snaar JEM, Teeuwisse WM, Versluis MJ, van Buchem MA, Kan HE, Smith NB, Webb AG (2010) Improvements in high-field

- localized MRS of the medial temporal lobe in humans using new deformable high-dielectric materials. *NMR Biomed* 24:873–879
31. Talagala SL, Ye FQ, Ledden PJ, Chesnick S (2004) Whole-brain 3D perfusion MRI at 3.0 T using CASL with a separate labeling coil. *Magn Reson Med* 52:131–140
 32. van Gelderen P, de Zwart JA, Starewicz P, Hinks RS, Duyn JH (2007) Real-time shimming to compensate for respiration-induced B0 fluctuations. *Magn Reson Med* 57:362–368
 33. Blamire AM, Rothman DL, Nixon T (1996) Dynamic shim updating: a new approach towards optimized whole brain shimming. *Magn Reson Med* 36:159–165
 34. Jahanian H, Noll DC, Hernandez-Garcia L (2011) B₀ field inhomogeneity considerations in pseudo-continuous arterial spin labeling (pCASL): effects on tagging efficiency and correction strategy. *NMR Biomed*. doi:[10.1002/nbm.1675](https://doi.org/10.1002/nbm.1675)
 35. Günther M, Oshio K, Feinberg DA (2005) Single-shot 3D imaging techniques improve arterial spin labeling perfusion measurements. *Magn Reson Med* 54:491–498